Anomalous transport properties in topological materials

Yan Sun[#], Jonathan Noky, Qiunan Xu, Wujin Shi, Yang Zhang, Enke Liu, Claudia Felser

Our research interest is to understand the topological and transport properties of materials based on topological band theory, symmetry analysis, transport theory, and experimental collaborations. A high anomalous Hall conductivity and large anomalous angle were observed in $Co_3Sn_2S_2$ owing to enhancements arising from Weyl point and nodal-line band structures. The topological state of $Co_3Sn_2S_2$ – as a magnetic Weyl semimetal – was verified via both ARPES and STM measurements. Antiferromagnets with zero net magnetization entail substantially fast spin dynamics; consequently, it would be interesting to obtain strong anomalous transport signals along with a topological band structure and an antiferromagnetic magnetic structure. Through symmetry analysis of the Berry curvature, it was determined that the global Berry phase in the whole Brillouin zone can entail a non-zero finite value for an antiferromagnet without combined time-reversal and inversion (or translation) symmetry. Such a collinear antiferromagnetic structure can be obtained via symmetry breaking at magnetic and non-magnetic sites connecting two magnetic sublattices. Furthermore, although the anomalous Hall effect and anomalous Nernst effect share the same symmetry requirement, their detailed relations to the electronic structure are different. Specifically, the anomalous Nernst effect is more sensitive to the first derivative of the anomalous Hall effect with respect to chemical potential; therefore, the anomalous Nernst effect can be used to detect topological band structures away from, especially above, the Fermi level. Notably, such band structures cannot be observed based on only the anomalous Hall effect and ARPES. Owing to time-reversal symmetry, linear responses such as the anomalous Hall effect and optical Hall effect are forbidden, and the signals of second-order non-linear responses can dominate in cases without inversion symmetry. With this understanding, we propose an optical method for identifying the chiral topological band structure in chiral crystals, which, thus far, could only be identified via surface Fermi arc detection.

The interplay between electromagnetic response and symmetry breaking is crucial in understanding the electrical and optical transport properties of quantum materials. In topological materials, Berry curvature is a fundamental parameter affecting topological charges and related properties. We aim to understand such materials based on the electronic band structures, Berry curvature, symmetry analysis, and electromagnetic response theories.

Giant AHE in magnetic Weyl semimetal $Co_3Sn_2S_2$. Magnetic Weyl semimetals (MWSMs) can be constructed using multi-layered quantum anomalous Hall insulators (QAHIs). From this perspective, MWSMs can considered to entail a 3D QAHE, and therefore, magnetic layer materials exhibiting a strong AHE and low charge carrier density are promising candidate for MWSMs. In collaboration with Liu et al., we observed a strong AHE in a layered magnetic semimetal, $Co_3Sn_2S_2$[1]. Notably, the anomalous Hall conductivity (AHC) and anomalous Hall angle (AHA) reached up to 1130 S/cm and 20%, respectively, owing to an enhanced Berry curvature from the Weyl bands and low charge conductivity (Fig. 1(a-c)). This was first 3D material with both a large AHC and AHA. Upon observing a good agreement between transport and theoretical results [1, 2], our collaborators Chen et al. and Beidenkopf et al. performed direct electronic

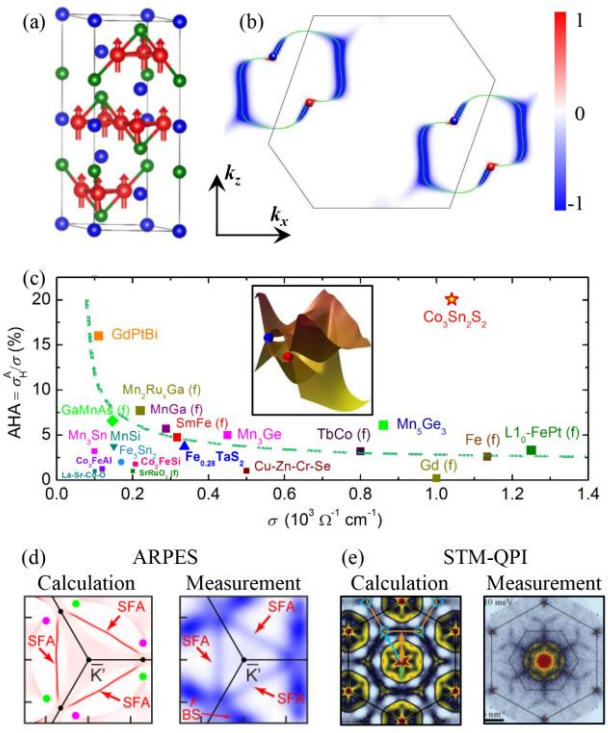

Fig. 1: (a) Lattice and magnetic structures of $Co_3Sn_2S_2$. (b) Berry curvature in $Co_3Sn_2S_2$. (c) Comparison of our σ_{HA}-dependent AHA results and previously reported data for other AHE materials. (d-e) Comparison between calculated surface Fermi arcs and experimental measurement.

band structure observations, and the predicted Weyl points and Fermi arcs were confirmed by both ARPES and STM measurements (Fig. 1 (d-e)) [3-4], making $Co_3Sn_2S_2$ the first experimentally verified MWSM.

AHE in collinear magnetic structure with vanishing magnetic moments. From the symmetry point of view, it is easy to understand that ferromagnets can exhibit the AHE, and a topological band structure can strongly enhance the magnitude of such an anomalous response. Similarly, the occurrence of the AHE and other related physical responses in systems without a net magnetic moment is also interesting. The observation of the AHE in the non-collinear antiferromagnet Mn_3Ge/Sn suggests that such phenomena are allowed owing to the absence of two sublattices, such as in collinear antiferromagnets. These results motivated us to extend this idea to collinear magnetic systems without a net magnetic moment. We found that it is possible to attain a non-zero finite AHE by breaking the inversion or translation symmetries related to two magnetic sublattices (see Fig. 2). Specifically, this can be achieved by breaking the symmetries at magnetic or non-magnetic positions. We proposed a model material, Ti_2MnAl [5], for the former case. Because Ti_2MnAl contains Weyl point band structures, its AHE and anomalous Nernst effect can reach up to ~500 S/cm and ~1.5 $A \cdot m^{-1}K^{-1}$, respectively. Moreover, since both inversion and time-reversal symmetry are broken in Ti_2MnAl, the generation of an intrinsic bulk spin–orbital torque in Ti_2MnAl is also possible.

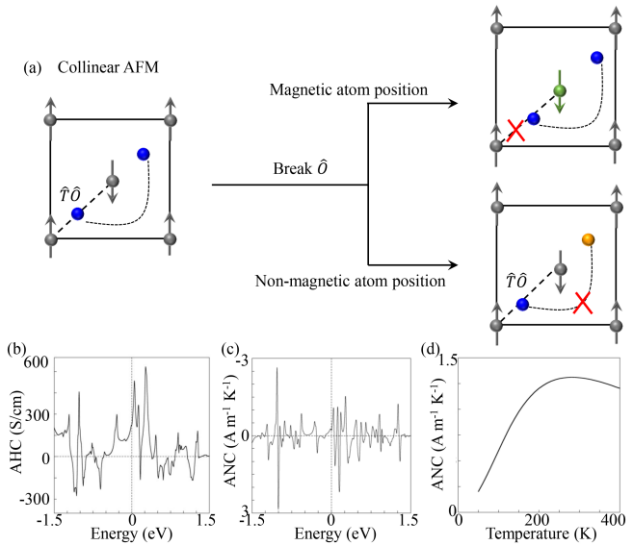

Fig. 2: (a) Schematic of symmetry breaking to attain collinear AFM AHE. (b-d) AHC and ANC in the model material Ti_2MnAl.

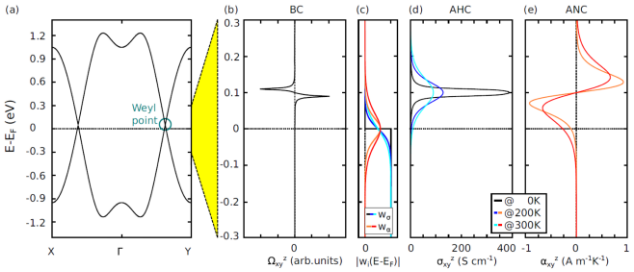

Fig. 3: (a-c) (a) Schematic of the band structure with Weyl points above the Fermi level. (b) Berry curvature at fixed energy integrated over the whole Brillouin zone. (c) Weighting functions for the AHC and ANC. (d) AHC with a very small value at the Fermi level. (e) Anomalous Nernst conductivity with a finite value at the Fermi level.

Characterization of topological band structures away from the Fermi level by the anomalous Nernst effect. Resolving the structure of energy bands in transport experiments is a major challenge in condensed matter physics and material science. Sometimes, however, traditional electrical conductance or resistance measurements only provide extremely small signals, thereby hindering the ability to obtain direct band structure information. A thermoelectric signal is more sensitive to the first derivative of the electrical characteristics with respect to energy, rather than to the electrical characteristics themselves. Presently, the AHE is a common means for accessing the Berry curvature directly via measurements, but the corresponding signals can be too small to be detected when the topological features of the band structure lie excessively far away from the Fermi level. Thus, we proposed the investigation of topological-band-structure features by using the ANE, which is related to the derivative of the AHE with respect to energy, as presented in Fig. 3. Through this method, signatures that are elusive in AHE measurements become resolvable [6]. We proposed two real Heusler compounds, Co_2FeX (where X = Ge, Sn), which should exhibit this property, with topological nodal lines that are ~100 meV above the Fermi level. This suggests that a magnetic topological band structure that is away from the Fermi level can generate a strong thermoelectric signal, in spite of the electronic transport signal being weak.

Identification of the chirality of a chiral topological semimetal by second-order non-linear optical responses. The chirality of chiral multi-fold fermions in reciprocal space is related to the chirality of crystal lattice structures in real space. For same compounds having opposite curability, the bulk electronic band structures are identical (see Fig. 4). Thus far,

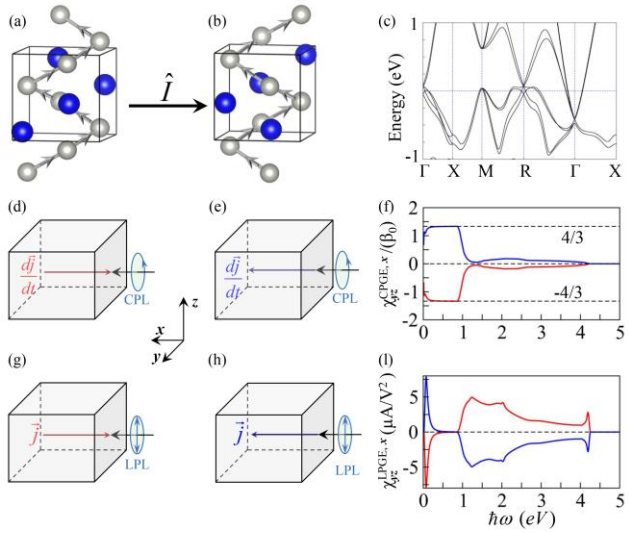

Fig. 4: Crystal lattice structures of RhSi semimetals with opposite chiralities in (a-b) have identical band structures in (c). For a given input polarized light, both the circular photogalvanic effects in (e-f) and the shift current (g-l) exhibit opposite signs.

differences among such compounds were only observed via surface Fermi arc detection using ARPES and STM. Based on second-order non-linear response theory and symmetry analysis, we proposed a strategy for the detection and identification of the chirality of multi-fold fermions via optical transport [7]. Chiral crystals related to inversion operations cannot be made to overlap with each other via any experimental operation. Moreover, chiral multi-fold fermions within such crystals host opposite chiralities corresponding to a given ***k*** point. A change in chirality is indicated by a corresponding change in the sign of the second-order charge current dominated by chiral fermions (see Fig. 4). This property can be exploited to study the relationship between chiralities in reciprocal and real spaces by bulk transport.

Database development for the material transport properties. It is crucial to fully understand the transport properties of materials and discover materials that host strong electromagnetic responses. However, such large-scale screening is experimentally impractical. On the contrary, this is, in principle, theoretically and computationally much more straightforward. With given crystal and magnetic structures as inputs, based on electronic band structure, symmetry analysis, quantum response theories, and high-throughput calculations, we developed databases for the AHE, ANE, and magneto-optical effect in Heusler magnetic materials and for the spin Hall effect and second-order non-linear optical effect in non-magnetic materials (see Fig. 5(a)) [8-9].

Through statistical analyses of the databases, we observed a strong and unexpected relation between the magnitude of the linear responses (including SHE, AHE, ANE, and magneto-optical effect) and crystalline symmetry, which is typically associated with mirror-symmetry-protected nodal lines in the band structure. This also provides a clear understanding of the benchmark SHE-exhibiting Pt materials, whose high SHC is due to the mirror-symmetry-protected nodal lines corresponding to the (110) plane (see Fig. 5 (b-c)). Similarly, the higher AHC in cubic regular Heusler compounds compared with that in inverse Heusler compounds is due to the mirror-symmetry-protected nodal lines (see Fig. 5(d)).

Vision 1: QAHE in 3D. In the last decade, owing to the experimental realization of non-zero-integer plateaus in both magnetic doped TIs and intrinsic magnetic compounds, substantial progress has been achieved in studying the QAHE. Magnetic topological semimetals, such as those exhibiting nodal lines or WSMs, can host strong anomalous linear responses corresponding to the AHE, ANE, and magneto-optical effects. The magnetic ordering temperature of 3D materials is generally higher than that of 2D systems. Hence, in 3D magnetic topological materials, the intrinsic contribution from the Berry curvature can maintain a robust and strong response signal over a large temperature range before the magnetic phase transition.

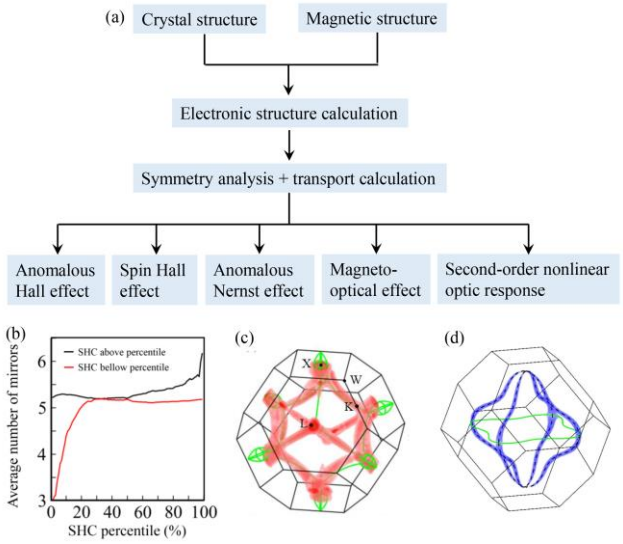

Fig. 5: (a) Schematic of workflow of database construction. (b) Average number of mirrors for materials with SHC above a percentile and below the percentile as a function of the percentile. (c) Mirror-plane(m_{110})-protected nodal lines contribute to the high SHC in Pt. (d) Mirror-plane(m_{100} and m_{010})-protected nodal lines contribute to the high AHC in Co_2MnGa with the magnetic moment set along z.

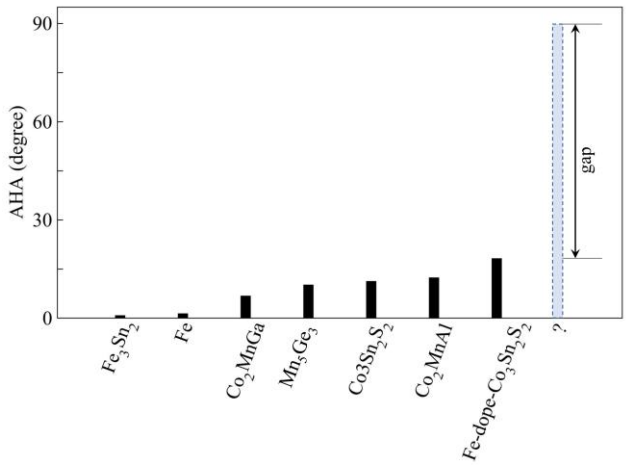

Fig. 6 Comparison of the AHA for known, typical 3D magnetic materials. The ideal upper limit of 90° has still not been reached in real materials. The data are from Ref. [1, 10-14].

The AHA can be employed to measure the topological contribution to the AHE. The intrinsic contribution of the AHA in 3D strong-AHE materials, such as $Co_3Sn_2S_2$ and nodal Co_2MnGa/Al, can reach up to ~20% (~11°). With an optimized combination of intrinsic and extrinsic contributions, the AHA in $Co_3Sn_2S_2$ can reach up to ~30% (~18°) within a small temperature range. However, these AHA values are still substantially lower than the upper limit of 90° (see Fig. 6). Therefore, in principle, there is still a clear and large gap between ideal models and real materials. The ideal case is the 3D-QAHE, whereby a dissipation-free strong AHE is expected.

Vision 2: QAHE in AFM. The AHE was theoretically proposed for both collinear and non-collinear AFMs via the breaking of joint time-reversal and space-group symmetry, which changes the sign of the Berry curvature, and some of such phenomena were experimentally observed recently in both collinear and non-collinear AFMs. In principle, this symmetry-based understanding can be extended to both 2D and 3D insulating systems with non-zero-integer plateaus (see Fig. 7). Because the dynamics of magnetic moments in AFMs are much faster than those in ferromagnets, the QAHE in AFMs is promising for the development of new types of fast dynamic quantum spintronic devices.

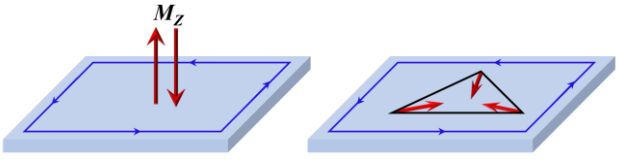

Fig. 7: Schematic of QAHE in AFMs with collinear and non-collinear magnetic structures.

Vison 3: Manipulation of quantum phase transitions by spin–orbital torque. Spin–orbital torque (SOT) is a promising means for developing future memory devices by controlling the magnetization orientation via electrical current. In contrast to a magnetic field, the torque on different local sites can be different or even opposite; this provides additional freedom to tune the magnetic structure. Two different effects are referred to as SOT: One is the torque generated in heavy-metal/FM heterostructures owing to the SHE and interface-induced symmetry breaking. The spin current generated from the SHE can flow in the FM and exert torque via the spin-transfer torque mechanism. The other is based on intrinsic bulk inversion and time-reversal symmetry breaking.

All topological states can be understood based on symmetry-protected topological charges. A SOT can arise in topological systems with broken time-reversal and inversion symmetry; this provides an effective strategy to tune quantum responses and quantum phase transitions. The SOT related to the QAHE is also expected to lead to some interesting phenomena, whereby the inversion symmetry breaking in the QAHE can be obtained intrinsically via the interface effect with a substrate or QAHE insulators without inversion symmetry. A non-zero SOT in the QAHE can be used to vary the bandgap and manipulate a topological phase with the variation of the chiral Chern number from C to $-C$ through 0. In a system with broken inversion and time-reversal symmetry, the SOT can be used to tune the position and chirality of Weyl points, in addition to tuning the shape and chirality of surface Fermi arcs. One extreme result is that if two opposite Weyl points coincide, it can lead to a full-gap 3D-QAHE or magnetic insulator.

References

[1]* *Giant anomalous Hall effect in a ferromagnetic kagome-lattice semimetal, E. Liu, Y. Sun, N. Kumar, L. Muechler, A. Sun, L. Jiao, S. Yang, D. Liu, A. Liang, Q. Xu, J. Kroder, V. Süß, H. Borrmann, C. Shekhar, et al., Nat. Phys.* ***14*** *(2018) 1125.*

[2]* *Topological surface Fermi arcs in the magnetic Weyl semimetal $Co_3Sn_2S_2$, Q. Xu, E. Liu, W. Shi, L. Muechler, J. Gayles, C. Felser, and Y. Sun, Phys. Rev. B* ***97*** *(2018) 235416.*

[3]* *Magnetic Weyl semimetal phase in a Kagomé crystal, D. Liu, A. Liang, E. Liu, Q. Xu, Y. Li, C. Chen, D. Pei, W. Shi, S. Mo, P. Dudin, et al., Science* ***365*** *(2019) 1282.*

[4]* *Fermi-arc diversity on surface terminations of the magnetic Weyl semimetal $Co_3Sn_2S_2$, N. Morali, R. Batabyal, P. K. Nag, E. Liu, Q. Xu, Y. Sun, B. Yan,*

*C. Felser, N. Avraham, and H. Beidenkopf, Science **365** (2019) 1286.*

[5] *Prediction of a magnetic Weyl semimetal without spin-orbit coupling and strong anomalous Hall effect in the Heusler compensated ferrimagnet Ti_2MnAl, W. Shi, L. Muechler, K. Manna, Y. Zhang, K. Koepernik, R. Car, J. Brink, C. Felser, and Y. Sun, Phys. Rev. B **97** (2018) 060406(R).*

[6]* *Characterization of topological band structures away from the Fermi level by the ANE, J. Noky, J. Gooth, C. Felser, and Y. Sun, Phys. Rev. B **98** (2018) 241106(R).*

[7]* *Optical method to detect the relationship between chirality, Y. Sun, Q. Xu, Y. Zhang, C. Le, and C. Felser, Phys. Rev. B **102** (2020) 104111.*

[8]* *Giant anomalous Hall and Nernst effect in magnetic cubic Heusler compounds, J. Noky, Y. Zhang, J. Gooth, C. Felser, and Y. Sun, npj Com. Mater. **6** (2020) 77.*

[9]* *Comprehensive scan for nonmagnetic WSMs with nonlinear optical response, Q. Xu, Y. Zhang, K. Koepernik, W. Shi, J. Brink, C. Felser, and Y. Sun, npj Com. Mater. **6** (2020) 32.*

[10] *Massive Dirac fermions in a ferromagnetic kagome metal, L. Ye, M. Kang, J. Liu, F. Cube, C. R. Wicker, T. Suzuki, C. Jozwiak, A. Bostwick, E. Rotenberg, D. Bell, et al., Nature **555** (2018) 638.*

[11] *Crossover Behavior of the Anomalous Hall Effect and Anomalous Nernst Effect in Itinerant Ferromagnets, T. Miyasato, N. Abe, T. Fujii, A. Asamitsu, S. Onoda, Y. Onose, N. Nagaosa, and Y. Tokura, Phys. Rev. Lett. **99** (2007) 086602.*

[12]* *From Colossal to Zero: Controlling the Anomalous Hall Effect in Magnetic Heusler Compounds via Berry Curvature Design, K. Manna, L. Muechler, T. Kao, R. Stinshoff, Y. Zhang, J. Gooth, N. Kumar, G. Kreiner, K. Koepernik, R. Car, et al., Phys. Rev. X **8** (2018) 041045.*

[13] *Giant room temperature anomalous Hall effect and tunable topology in a ferromagnetic topological semimetal Co_2MnAl, P. Li, J. Koo, W. Ning, J. Li, L. Miao, L. Min, Y. Zhu, Y. Wang, N. Alem, C. Liu, et al., Nat. Comm. **11** (2020) 3476.*

[14] *33% Giant Anomalous Hall Current Driven by Both Intrinsic and Extrinsic Contributions in Magnetic Weyl Semimetal $Co_3Sn_2S_2$, J. Shen, Q. Zeng, S. Zhang, H. Sun, Q. Yao, X. Xi, W. Wang, G. Wu, B. Shen, Q. Liu, and Enke Liu, Adv. Funct. Mater. **30** (2020) 2000830.*

ysun@cpfs.mpg.de